



ISSN: 0975-833X

Available online at <http://www.journalcra.com>

INTERNATIONAL JOURNAL
OF CURRENT RESEARCH

International Journal of Current Research
Vol. 14, Issue, 04, pp.21155-21160, April, 2022

DOI: <https://doi.org/10.24941/ijcr.43382.04.2022>

RESEARCH ARTICLE

INFLUENCE OF VORTEX STRUCTURES AND TURBULENCE ON THE CARBON NANOPARTICLES DISPERSION

¹Keita, N. S., ²Mehel, A., ³Murzyn, F., ⁴Taniere, A., ¹Diourte, B.

¹Physics Department, Faculty of Science and Technology Bamako, USTTB, Mali

²Department of Mechanical and Environmental Engineering, Air Quality and Depollution Group, ESTACA Paris Saclay Campus, 78180, Montigny-le-Bretonneux, France

³Department of Mechanical and Environmental Engineering, Air Quality and Depollution Group, ESTACA West Campus, 53000, Laval, France

⁴University of Lorraine, CNRS, LEMTA, F-54000, Nancy, France

ARTICLE INFO

Article History:

Received 12th January, 2022

Received in revised form

08th February, 2022

Accepted 20th March, 2022

Published online 28th April, 2022

Keywords:

Nanoparticles dispersion, turbulence, Air quality, RANS, Cylinder wake flow.

*Corresponding author:

Keita, N. S.,

ABSTRACT

This report aims to make a state the nanoparticles resulting from transportation systems lead to degradation of air quality causing damage to human health. The dynamics of these ultrafine particles is strongly related to the flow characteristics. The present work is devoted to numerical simulation of the two phase flow (air + nanoparticles) which develops downstream of a circular cylinder of a diameter $d=2.5$ cm. The goal is to provide a better understanding of the influence of turbulence and vortex structures created in the wake of a cylinder on the dispersion of the carbon nanoparticles. The studied flow ($Re = 9300$) was solved with the URANS model coupled with a lagrangian particle tracking. On the one hand, the results show that the nanoparticles tend to be located in the street of the vortices created by the wake of the cylinder. On the other hand, it is shown that the turbulence allows a wider dispersion compared to the case where no turbulence was considered.

Copyright © 2022. Keita et al. This is an open access article distributed under the Creative Commons Attribution License, which permits unrestricted use, distribution, and reproduction in any medium, provided the original work is properly cited.

Citation: Keita, N. S., Mehel, A., Murzyn, F., Taniere, A., Diourte, B., "Influence of vortex structures and turbulence on the carbon nanoparticles dispersion", 2022. International Journal of Current Research, 14, (04), 21155-21160.

INTRODUCTION

Improving air quality has become a major issue, particularly in terms of public health and environment. According to the World Health Organization (WHO), air pollution is responsible for 7 million premature deaths per year worldwide⁽¹⁾. This is partly due to the deterioration of air quality. This is at the origin of the aggravation of allergies, the development of cardiovascular and pulmonary diseases in particular. Among victims, the elderly and children are the most exposed. According to UNICEF⁽²⁾, 300 million children worldwide live in a place where outdoor air pollution is six times higher than international standards. At the same time, if we take into account the costs of repairing and maintaining buildings and monuments whose deterioration is linked to this pollution, the overall cost of this pollution will be around 1% of GDP (Gross Domestic Product) by 2060, according to the OECD (Organization for Economic Cooperation and Development)⁽³⁾. There are different sources of pollution. Among these, road transport is a major contributor, particularly in urban areas. The main pollutants emitted are ultrafine particles (UFP). Thus, in a recent report, Roumegas and Saddier (2016) indicate that in France the road sector is responsible for the emissions of NO_x, PM₁₀ and PM_{2.5} up to 54%, 16% and 19%, respectively⁽⁴⁾. If we want to limit human exposure to these pollutants, particularly harmful in a microenvironment such as the passenger compartment of a vehicle or bus, it is necessary to better understand their dynamics from the exit of the exhaust and their interaction with the surrounding flow. The ultimate objective is to reduce/limit their infiltration into the following vehicles by both passive and active means.

Thus, the improvement of our state knowledge on the spatial and temporal evolutions of the concentrations of nanoparticles from the exhaust of a vehicle in connection with wake flow is of major importance. Indeed, the dynamics of these ultrafine particles are strongly influenced by the structure of the flow and in particular by the presence of turbulent vortices. Dispersal of particles by turbulence has been shown to be a predominant mechanism (Mehel *et al.* 2010). It is therefore essential to characterize the structure of wake flow and to quantify the interaction of particles with this flow. Some studies have investigated these interactions by conducting dispersal measurements in the wake of a vehicle. For example, Carpentieri and Kumar (2011) made measurements using a grid mounted on the rear of a vehicle in the near wake area with a total of 9 sensors placed at distances ranging from 0.45m to 0.8m from the bumper. Their study gives an idea of the dynamics of particle dispersion but the area covered remains very limited. In view of the difficulties of having a large number of measurements of concentrations at different locations in the wake of a vehicle, some work has opted for the study of the dispersion of ultrafine particles in the wake of model vehicles in wind tunnels. For example, Kanda *et al.* (2006) worked with two types of vehicle models (a car and a truck). They showed that the exhaust gases dispersion increases significantly in the wake in the presence of the vehicle compared to the case without a vehicle. Carpentieri *et al.* (2012) investigated the influence of the boundary layer on the bottom through a mobile floor. They showed that the dispersion of ultrafine particles in the near wake is attenuated while it is increased in the far wake. However, both studies used a tracer gas in the wake to simulate particle dispersion. Unlike solid particles, which can undergo deposition and agglomeration mechanisms (Carpentieri *et al.* 2011), the latter does not undergo transformation, which alters their dispersion dynamics (Mehel and Murzyn 2015). The numerical work presented is in this context. It is then a question of injecting solid particles instead of tracer gases. In particular, the influence of vortex structures and turbulence on the dispersion of carbon nanoparticles is sought to be finely characterized. For this, our approach is initially concerned with the flow that develops in the wake of a simple obstacle and well referenced in the literature: the cylinder. Our cylinder has a diameter of 2.5cm and the upstream speed is $U=5.56$ m/s for a number of Reynolds $Re=9300$. After the presentation of the conditions of our numerical modelling (choice of the turbulence model, definition of the mesh, etc.), the main results will be presented focusing particularly on the concentration fields at different distances downstream of the cylinder. The last part will be devoted to the synthesis of the results and a presentation of the perspectives and future developments. In particular, for our next step, the cylinder will be replaced by a simplified vehicle geometry (Ahmed's body) in order to get even closer to a real situation for which our results can be compared with experimental data obtained in wind tunnel.

Numerical method: Our study is based on a 2D simulation of the flow with an Eulerian approach type URANS (Unsteady Reynolds Average Navier-Stokes) combined with a lagrangian monitoring of the particles. Our simulations were carried out using the commercial code Fluent (version 16.1). The statistical resolution of the Navier-Stokes averaged equations of equation (Eq. 1) reveals new terms, namely the double correlations that form the Reynolds tensor. Thus, for the resolution of the turbulence represented by this double correlation, we opted for the Reynolds Stress Model (RSM) associated with a near-wall treatment type Enhanced Wall Treatment (EWT). This choice stems from a preliminary comparative study with the existing literature concerning in particular two characteristic parameters related to the topology of the monophasic flow of the wake cylinder: the separation angle θ and the recirculation length measured by the cylinder diameter (noted L_r/d). The main results of this study are presented in Table 1. Analysis of the latter shows that our results are in good agreement with various experimental studies ^{(5), (6)}. Norberg *et al.* (1994) ⁽⁵⁾ stated that L_r/d of the downstream flow of the cylinder decreases from 1.8 to 0.8 when the Reynolds number increases between 1500 and 15000. Similarly, Perrin (2005) [6] found that the angle of detachment remained constant when Re went from 1000 to 100000 (Table 1).

Table 1. Calibration of the numerical model with existing literature

	L_r/d	θ	Re
Norberg <i>et al.</i> (1994) [5]	1,8 à 0,8	-	1500< Re <15000
Perrin Thesis (2005) [6]	-	80	1000< Re <100000
Presentstudy	0,9	81	$Re= 9300$

$$\rho \frac{\partial \bar{u}_i}{\partial t} + \rho \frac{\partial (\bar{u}_i \bar{u}_j)}{\partial x_j} = \rho \bar{F}_i - \frac{\partial \bar{P}}{\partial x_i} + \frac{\partial}{\partial x_j} [\bar{\tau}_{ij} - \rho \bar{u}_i' \bar{u}_j'] \quad (\text{Eq. 1})$$

$$\text{with } \bar{\tau}_{ij} = \mu \left[\frac{\partial \bar{u}_i}{\partial x_j} + \frac{\partial \bar{u}_j}{\partial x_i} \right]$$

The term $\rho \bar{u}_i' \bar{u}_j'$ is a constraint resulting from the turbulent agitation movement. This is Reynolds stress. The interaction of the nanoparticles with the turbulence of the flow is ensured by the EIM (Eddy-Interaction Model) model of the particles dispersion by turbulence. It is a stochastic model used to model turbulent flow fluctuations. It consists in generating fluctuating velocities of the carrier fluid respecting the local average turbulent intensity and kept constant for a given time [7]. The fluctuating velocity of the fluid seen by the particle noted by u_i^* is generated via the equation below:

$$u_i^* = G \sqrt{\langle u_i'^2 \rangle} \quad (\text{Eq. 2})$$

with $\sqrt{\langle u_i'^2 \rangle}$ the standard deviation of the mean value of fluctuating velocities and G a random number of the Gaussian distribution centered and reduced.

Geometry and Mesh: Figures 1 and 2 respectively represent the geometry and mesh of the study field with a zoom on the boundary layer mesh (Figure 2). Dimensional parameters for the study area were selected in accordance with the study by Nishino *et al.* (2008)⁽⁸⁾. The length between the cylinder center at the inlet and the outlet cylinder center of the domain are $L_i=10d$ and $L_o=20d$ respectively. The height of the domain is $H=10d$. Note U_∞ the infinite speed upstream, x the main direction of flow (horizontal axis) and y the vertical direction. The origin of the mark is taken as the middle of the cylinder at the coordinate point ($x=0, y=0$). In the boundary layer in the vicinity of the cylinder wall, 10 layers are created with a progression rate of 1.2 from the size of the first layer. Beyond, and within a radius of 7cm, the size of the elements is 2mm. Far from the wall, the size of the mesh is 5mm. The total number of elements is 28402.

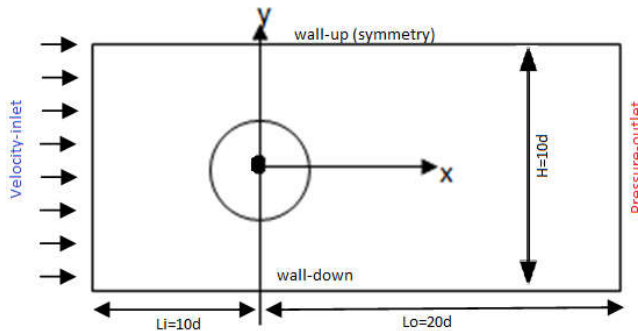


Figure 1: study field of geometry

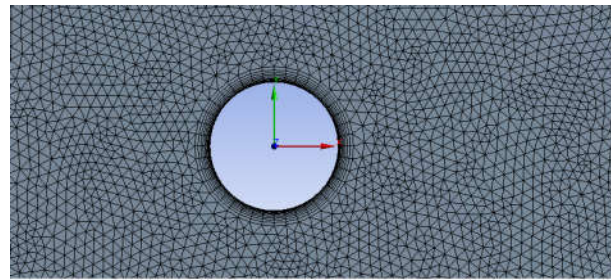


Figure 2: Domain Mesh

Simulation conditions: For the continuous fluid carrier phase, the inlet air velocity (velocity-inlet) is $U_\infty=5.56$ m/s corresponding to a Reynolds number $Re=9300$, where $d=25$ mm. The relative outlet pressure (pressure-outlet) is set at the standard atmospheric pressure ($P=101325$ Pa). Regarding the particles properties and injection, the injector simulating the exhaust pipe is located below the cylinder at a dimensionless position ($x/d=0$ and $y/d=-0.62$)⁽⁹⁾. The origin is taken at the cylinder center, x being the stream wise direction positive downstream and y being the vertical direction positive upward. We inject 1000 parcels of carbon nanoparticles with a diameter $d_p=10nm$ ($St=3\cdot 10^{-6}$) and a density $\rho_p=2000$ kg/m³ at each time step $\Delta t=10^{-4}$ s. The particles injection velocity is $u_{p,i}=6.875$ m/s with a mass flow rate of carbon nanoparticles $\frac{dm}{dt}=0.0625$ mg/s. This flow rate was calculated according to the standard EURO6 concerning the limitation levels of particles emitted by vehicles (4,5mg/km) and for an urban velocity of (50 km/h). Finally, each parcel represents $5.97\cdot 10^6$ carbon nanoparticles. The total iteration number is 2500. Brownian diffusion is not considered in this study.

RESULTS

The evaluation of the turbulence influence on nanoparticle dynamics was carried out by comparing the results obtained when the turbulence dispersion model (EIM) is activated with those for which it is not take into account. For effect of vortex structures on nanoparticles dispersion in the wake, we also simulated the flow with and without a cylinder while injecting the particles in the same position. This approach allows us to have a reference situation (without the presence of the cylinder, Figure 3a). Figures 3a-b-c represent the different positioning maps of carbon nanoparticles at time $t=0.25$ s colored by their residence time. In this study, residence time is the residence time of nanoparticles in the computational domain. It is highly variable and depends essentially, for a given particle size, on their interaction with turbulent vortex structures. Figure 3a represents the reference case (without the presence of the cylinder). Figure 3b corresponds to the results with cylinder when the dispersion model (EIM) is not activated and Figure 3c if this model is activated.

The overall analysis of Figures 3a to 3c shows that the flow structure has a strong influence on nanoparticles dynamics. Indeed, without the presence of the cylinder (Figure 3a), that is to say in the absence of the vortex structures, the nanoparticles tend to follow the longitudinal passing through the injection point with a lower residence time in the domain (maximum around 0.1s). For the case of cylinder presence, the nanoparticles are dispersed solely by the impact of the vortex structures that develop in the wake flow of the cylinder. The maximum values of residence time in this case is 0.24s. By activating the EIM model (Fig. 3c), we notice that the carbon nanoparticles diffuse more significantly in the wake of the cylinder. Furthermore, particles with a high residence time are found in the core of the vortices. This trends show that vortices trap carbon nanoparticles first at the periphery of vortices and then in their core. To develop our analysis, we also looked at the evolution of the carbon nanoparticles concentration in different vertical planes downstream of the cylinder for different distances x/d . When $1 < x/d < 10$, we will be considered the near wake cylinder. The far wake of a cylinder is associated with the case where $x/d > 10$. Figures 4, 5 and 6 represent the concentration profiles of as dimensionless concentrations (C^*). C^* is given by Eq 3:

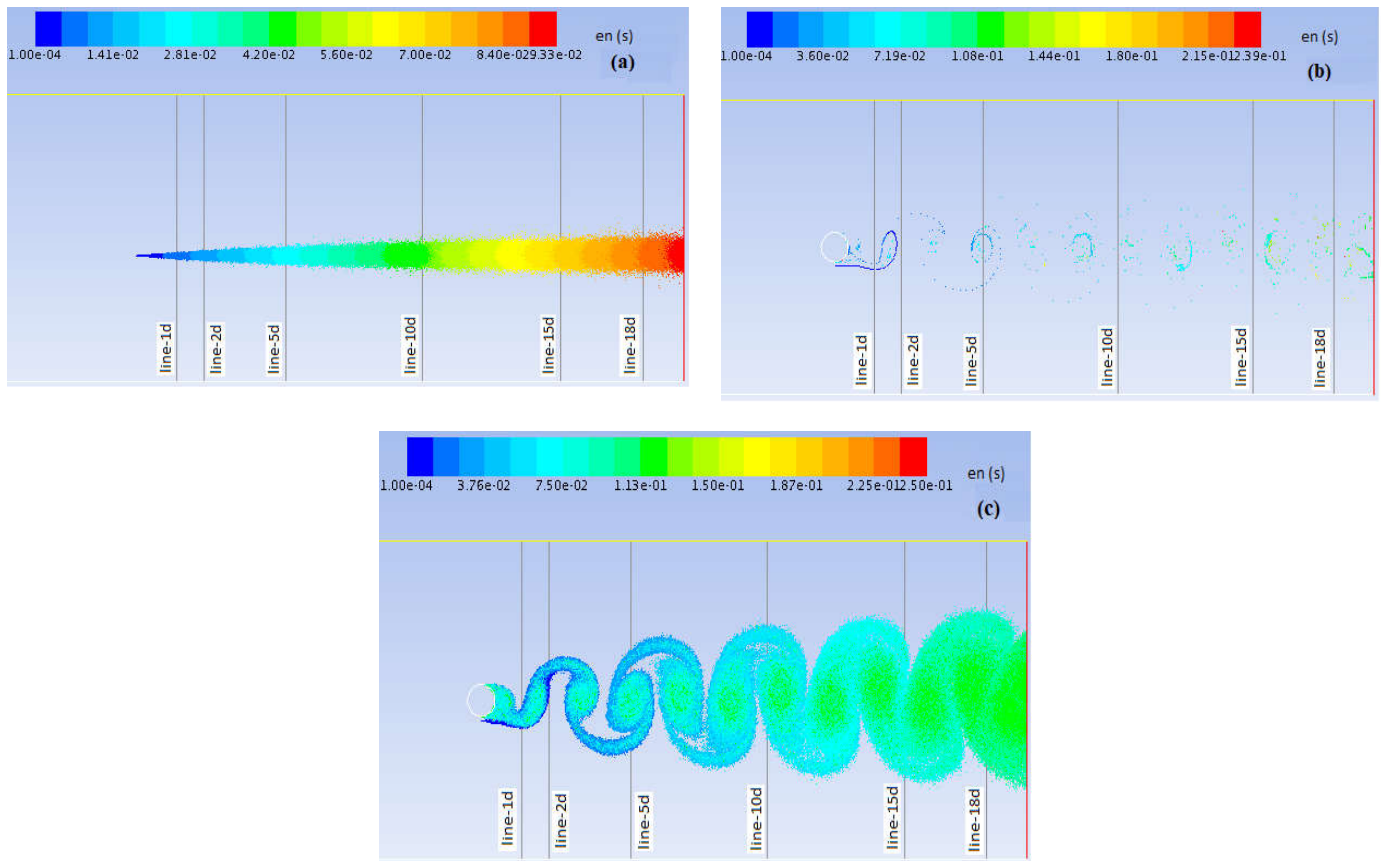


Figure 3. Contours of nanoparticle positions colored by their residence time: a) without cylinder with EIM; b) with cylinder and without EIM; c) with cylinder with EIM

$$C^* = C/C_{max} \quad (\text{Eq. 3})$$

where $C(\text{kg}/\text{m}^3)$ is the instantaneous concentration of particles and C_{max} is the maximum corresponding value of C .

As mentioned earlier (Figure 3), the first element that emerges from Figures 4, 5 and 6 is the demonstration of the decrease in the concentration of particles during the passage of the near wake to the distant wake, regardless of the configuration tested (with or without cylinder, EIM model enabled or not). In these figures, the lateral dispersion is represented by the widening of the curve at its base and the decrease in the amplitude of the peak concentration.

In Figure 4 (case without cylinder), in the absence of vortex structures, dispersion remains limited. It operates symmetrically around the injection position $y/d = -0.62$. Indeed, particles have a much important horizontal component of velocity than the vertical component. Figures 5a and 5b (with cylinder, EIM model not activated) and 6a and 6b (with cylinder, EIM model activated) provide information of the turbulence influence on concentration fields. When the EIM dispersion model is activated, it is noted that the dispersion of nanoparticles is more homogeneous and extensive (Figure 6) than when the EIM model is deactivated (Figure 5).

For example, the scatter field in $x/d = 18$ is found to be between $y/d = -2.5$ and $y/d = 2.5$ (Figure 6b) while this feature is not as marked on Figure 5b where the scatter is between $y/d = -1$ and $y/d = 1$. On the other hand, there is a much more pronounced peak in $x/d = 5$ in Figure 5b, which indicates the passage of a charged particle tourbillon as shown in Figure 3c. In the near wake ($x/d = 1$), Figures 5 and 6 show that the particles are simply driven by the flow, the dispersion (base of the peak concentration) being reduced. This is due to the proximity of the measurement to the injector position. In $x/d = 2$, when the EIM model is not enabled, the fat concentration is zero (Figure 5a). The reason for this is that, at this location, you are in a zone of unleashed vortex structures coming from the recirculation zone. The length of the cylinder wall is 0.0225m (Table 1).

This release occurs alternately on either side of the central axis ($y/d = 0$) which explains that the line $x/d = 2$ records the passage of particles in a sinusoidal manner. The final time of our simulation ($t = 0.25\text{s}$), is in the ascent phase of structures containing nanoparticles above the center line in $y/d = 0$ (Figure 3b). To characterize the effects of tourbillon structures, the results associated with the presence of the cylinder are compared with those obtained in the absence of the cylinder. For this, the analysis of Figures 5 and 6 shows that the vortex structures lead to an increased dispersion on both sides of the Von-Karman street. Indeed, we notice peaks in concentrations on both sides in relation to the center of the cylinder which is at $y/d = 0$. On the other hand, the nanoparticles at the center of the vortices are those that have a greater residence time (Figure 3c). So this leads us to think that they were trapped in these vortex that make up Von Karman Street.

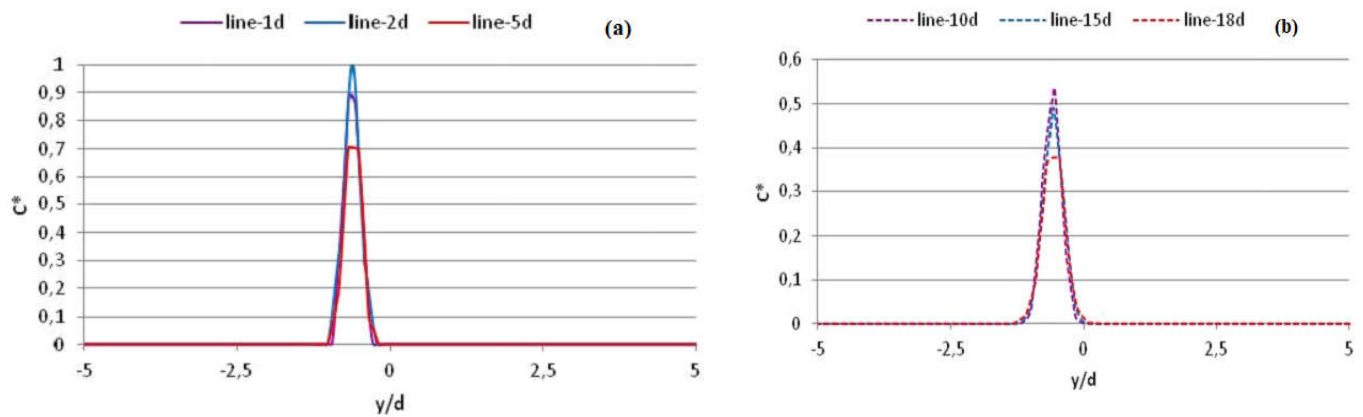


Figure 4. Evolution of the nanoparticles concentration at the cylinder presence: a) domain of the near wake; b) domain of the far wake

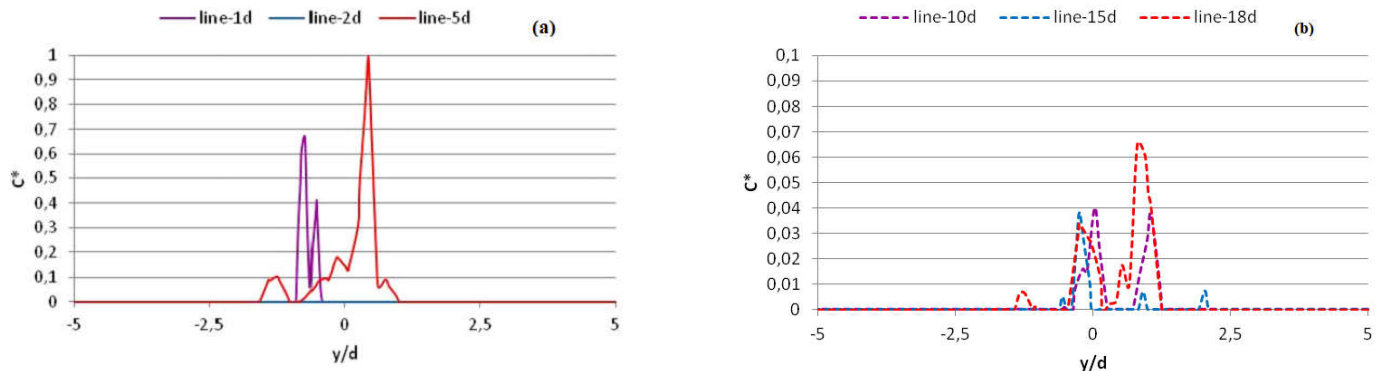


Figure 5. Evolution of the nanoparticles concentration in the cylinder wake without taking into account the turbulent dispersion model (EIM): a) near wake; b) distant wake

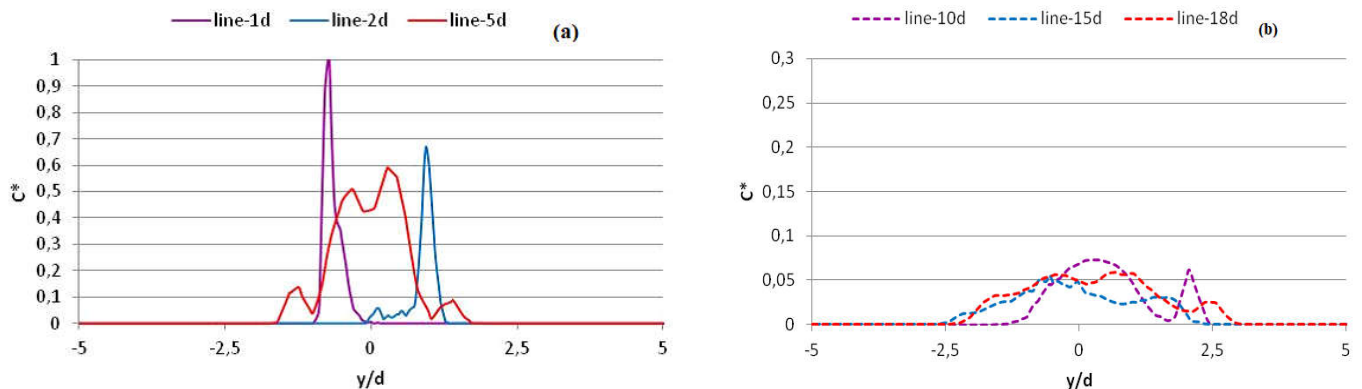


Figure 6. Evolution of the nanoparticles concentration in the cylinder wake with consideration of the turbulent dispersion model (EIM): a) near wake; b) far wake

CONCLUSION

In this work, a numerical study of the solid nanoparticles dispersion in the wake of a cylinder is presented. Our interest has focused in particular on an analysis of the turbulent and vortex structures influence that develop in the wake on the capture and transport of these nanoparticles. Our results show that particles dispersion dynamics are strongly related to the structure in the wake flow. In particular, we highlight that particles can be trapped by wake vortices. The next work will be to simulate the dispersion of these same carbon nanoparticles in the wake of a traditionally used model of motor vehicle: Ahmed body. It is a simplified geometric model for which only the tilt angle of the rear bezel influences the wake flow topology. Our interest will focus in particular on a square Ahmed body to allow us a comparative study with experimental data acquired in wind tunnel.

Acknowledgement

University of Technical sciences and Technology of Bamako (Mali), ESTACA (France), University of Lorraine (France) are acknowledged for their financial and technical support.

REFERENCES

- Statistiques sanitaires mondiales 2012. Organisation Mondiale de la Santé. Genève, 2012. 978-92-4-256444-0.
- Résumé sur Assainissons de l'air pour les enfants. Unicef, 2016-pdf
- Les conséquences économiques de la pollution de l'air extérieur. L'ESSENTIEL STRATÉGIQUE. OCDE, juin 2016
- Roumégas J. L. et M. Saddier. Rapport d'évaluation des politiques publiques de lutte contre la pollution de l'air, Mai 2016.
- Mehel, A. A. Tanière, B. Oesterlé, J. R. Fontaine. The influence of an anisotropic Langevin dispersion model on the prediction of micro- and nanoparticle deposition in wall-bounded turbulent flows, *Journal of Aerosol Science*, 2010, 41, 729-744.
- Carpentieri, M. and P. Kumar. Ground-fixed and on-board measurements of nanoparticles in the wake of a moving vehicle. *Atmospheric Environment*, 2011, 45, 5837-5852.
- Kanda, I. K. Uehara, Y. Yamao, Y. Yoshikawa, T. Morikawa. A wind-tunnel study on exhaust gas dispersion from road vehicles—Part I: Velocity and concentration fields behind single vehicles. *Journal of Wind Engineering and Industrial Aerodynamics*, 2006 94, 639-658.
- Carpentieri, M. P. Kumar, A. Robins. Wind tunnel measurements for dispersion modelling of vehicle wakes. *Atmospheric Environment*, 2012, 62, 9-25.
- Mehel A. and F. Murzyn, Effect of air velocity on nanoparticles dispersion in the wake of a vehicle model: Wind tunnel experiments, *Atmospheric Pollution Research* 6, July 2015, Pages 612-617
- Norberg. C. LDV measurements in the near wake of a circular cylinder. In *Proceedings of the 1998 Conference on Bluff Body Wakes and Vortex-Induced Vibration* (eds P. W. Bearman C. H. K. Williamson), pages 1–12, Washington, DC, USA, 1998.
- Perrin. R. Analyse physique et modélisation d'écoulements incompressibles instationnaires turbulents autour d'un cylindre circulaire à grand nombre de Reynolds. Thèse de doctorat de l'Institut National Polytechnique de Toulouse, 2005
- Mehel. A. Evolution spatio-temporelle d'un aérosol de nanoparticules : phase I. Etude de la déposition. Postdoc, décembre 2008
- Nishino, T. G. T. Roberts, X. Zhang. Unsteady RANS and detached-eddy simulations of flow around a circular cylinder in ground effect. *Journal of Fluids and Structures* 24 (2008) 18-33.
- Pope C. A.III, R. T. Burnett, M. C. Turner, A. Cohen, D. Krewski, M. Jerrett, S. M. Gapstur, and M. J. Thun. Lung Cancer and Cardiovascular Disease Mortality Associated with Ambient Air Pollution and Cigarette Smoke: shape of the Exposure–Response Relationships. *Environmental Health Perspectives*, 2010.
- Atkinson, R. W. G. W. Fuller, H. R. Anderson, R. M. Harrison, B. Armstrong, 2010. Urban ambient particle metrics and health: a time-series analysis. *Epidemiology* 21, 501-511.
- Brugge, D. J. L. Durant, C. Rioux, 2007. Near-highway pollutants in motor vehicle exhaust: a review of epidemiologic evidence of cardiac and pulmonary health risks. *EnvironmentalHealth* 6, 23.
